HHS Public Access

Author manuscript

Neuron. Author manuscript; available in PMC 2016 August 05.

Published in final edited form as:

Neuron. 2015 August 5; 87(3): 657–670. doi:10.1016/j.neuron.2015.06.037.

Functional system and areal organization of a highly sampled individual human brain

Timothy O. Laumann[1], **Evan M. Gordon**[1], **Babatunde Adeyemo**[1], **Abraham Z. Snyder**[1,2], **Sung Jun Joo**[3], **Mei-Yen Chen**[3], **Adrian W. Gilmore**[4], **Kathleen B. McDermott**[2,4], **Steven M. Nelson**[5,6], **Nico U.F. Dosenbach**[1], **Bradley L. Schlaggar**[1,2,7,8,9], **Jeanette A. Mumford**[10], **Russell A. Poldrack**[3,11,12,13], and **Steven E. Petersen**[1,2,4,9]

[1]Department of Neurology, Washington University School of Medicine, St. Louis, MO, USA, 63110

[2]Department of Radiology, Washington University School of Medicine, St. Louis, MO, USA, 63110

[3]Department of Psychology, University of Texas at Austin, TX, USA, 78712

[4]Department of Psychology, Washington University in St. Louis, MO, USA, 63110

[5]VISN 17 Center of Excellence for Research on Returning War Veterans, Waco, TX, USA, 76711

[6]Center for Vital Longevity, School of Behavioral and Brain Sciences, University of Texas at Dallas, Dallas, TX, 75235

[7]Department of Psychiatry, Washington University School of Medicine, St. Louis, MO, USA, 63110

[8]Departmen of Pediatrics, Washington University School of Medicine, St. Louis, MO, USA, 63110

[9]Department of Anatomy and Neurobiology, Washington University School of Medicine, St. Louis, MO, USA, 63110

[10]Center for Investigating Healthy Minds at the Waisman Center, University of Wisconsin-Madison, WI, USA, 53705

[11]Department of Neuroscience, University of Texas at Austin, TX, USA, 78712

[12]Imaging Research Center, University of Texas at Austin, TX, USA, 78712

[13]Department of Psychology, Stanford University, CA, USA, 94305

Summary

Corresponding Author: Timothy O. Laumann, **Corresponding Author's Contact Information:** Wash Univ Sch Med Dept of Neurol, 660 S Euclid Ave, Box 8111, St. Louis, MO 63110 USA, laumannt@wusm.wustl.edu, Phone: +1 314 362 3317, Fax: +1 314 362 2186.

The authors report no conflicts of interest.

Resting state functional MRI has enabled description of group-level functional brain organization at multiple spatial scales. However, cross-subject averaging may obscure patterns of brain organization specific to each individual. Here, we characterized the brain organization of a single individual repeatedly measured over more than a year. We report a reproducible and internally valid subject-specific areal-level parcellation that corresponds with subject-specific task activations. Highly convergent correlation network estimates can be derived from this parcellation if sufficient data are collected – considerably more than typically acquired. Notably, within-subject correlation variability across sessions exhibited a heterogeneous distribution across the cortex concentrated in visual and somato-motor regions, distinct from the pattern of inter-subject variability. Further, although the individual's systems-level organization is broadly similar to the group, it demonstrates distinct topological features. These results provide a foundation for studies of individual differences in cortical organization and function, especially for special or rare individuals.

Introduction

The human brain exhibits a substantial degree of anatomic and functional variability across individuals. This fundamental observation has both frustrated and intrigued investigators who have sought to relate individual differences in brain organization to normal variability in behavior and cognition, as well as to the pathophysiology of disease (Devlin et al., 2007; Van Essen et al., 2007). Sophisticated strategies for transforming inter-subject anatomical variability into standard volumetric and, more recently, surface-based common spaces allow meaningful comparisons across individuals (Fischl et al., 1999; Fox et al., 1985). However, such transformations necessarily obscure individual variability in functional organization. Just as no single brain is representative of a population, no group-averaged brain represents a given individual. Furthermore, an observed pattern of functional brain organization in an individual may reflect persistent traits shaped by development and genetics, but may also relate to current state or environmental effects. Ultimately, accurate identification of brain-behavior relationships will require precise characterization of brain organization in individuals that takes into account both measurement error and intra-individual sources of variability.

Great advances recently have been made in describing group-average functional brain organization using resting state functional connectivity (RSFC). RSFC is based on the observation that the blood oxygen level dependent (BOLD) fMRI signal is correlated between spatially separated but functionally related regions of the brain (Biswal et al., 1995). Using this non-invasive technique, functional organization has been identified at the systems and areal level – two discrete scales of brain organization (Churchland et al., 1988). At the systems level, many investigators have used a variety of methods to produce increasingly comprehensive RSFC-based descriptions of distributed cortical and subcortical systems (Choi et al., 2012; Dosenbach et al., 2007; Doucet et al., 2011; Power et al., 2011; Yeo et al., 2011) that appear to correspond with functional systems coactivated by tasks (Power et al., 2011; Smith et al., 2009). At the areal level, (Cohen et al., 2008) have shown that RSFC exhibits abrupt transitions between cortical areas, i.e. regions of cortex that classically can be discriminated by multiple convergent properties including function,

architectonics, connectivity, and topographic mapping (Felleman et al., 1991). Based on this observation, the whole cortex has been divided into discrete functional parcels, some of which correspond to task activations and cytoarchitectonically-defined areas (Gordon et al., 2014b; Wig et al., 2014b; Yeo et al., 2014). Indeed, definition of cortical regions that segregate functional areas of this type should be an important first step in pursuing network-level analyses that reflect relevant neurobiological principles (Power et al., 2011; Smith et al., 2011; Wig et al., 2011). Thus, RSFC has enabled clear progress in the understanding of brain function and organization at multiple scales in groups of subjects, providing a powerful context for understanding brain function. However, these group-level analyses, which necessarily describe group-average data, provide only an approximate view of any individual's brain organization, potentially obscuring meaningful individual differences in cortical organization.

Here, we develop a detailed description of individual functional areal and systems brain organization, including how such organization differs from group-level estimates of organization. Importantly, precise estimates of individual functional brain organization can only be obtained by acquiring sufficient data to overcome sampling error and other sources of variability. RSFC studies commonly acquire only 5-10 minutes of scan time on each participant, based on recommendations given in past reports (Damoiseaux et al., 2006; Shehzad et al., 2009; Van Dijk et al., 2010). This quantity of individual data may be adequate for characterizing group-level patterns of functional brain organization and group-level differences. However, more recent reports have suggested that reliability is substantially improved with more than 10 minutes of data (Anderson et al., 2011; Birn et al., 2013; Hacker et al., 2013). Most dramatically, Anderson and colleagues (2011) have reported that at least 25 minutes of scan time and, in some cases, as much as 4 hours is needed to distinguish an individual from the group on the basis of RSFC. The total quantity of data required to accurately estimate whole-brain descriptions of functional organization in an individual remains an open question.

To address these considerations, we repeatedly studied one individual over more than a year, accumulating 14 hours of resting state fMRI, as part of an extensive phenotypic assessment of a single human. Using these data, we define a subject-specific areal parcellation and compare it against task activations acquired in the same subject. We then demonstrate the reliability and inter-session variability of correlation networks derived from this parcellation. Finally, we report the commonalities and idiosyncrasies of system topology, i.e. the specific spatial adjacencies of functional systems with respect to each other as identified by RSFC, in the individual as compared to a group of normal control subjects (and we further validated these observations in a second highly-sampled subject). This approach highlights the challenges that inter- and intra-subject variability bring to understanding functional brain organization. It also sets the stage, in this dataset, for relating longitudinal dynamics of brain function to behavioral and metabolic variability (detailed in Poldrack et al. (in revision)), and, more broadly, provides a model for the detailed characterization of functional brain organization in special or rare individuals using RSFC.

Results

Subject-specific areal parcellation

Evaluation of subject-specific RSFC-based parcellation—An individual subject parcellation was generated using data from 84 resting state sessions following the RSFC-gradient based procedure described in detail in (Gordon et al., 2014b) and (Wig et al., 2014b). In brief, this method uses spatial gradients in the similarity of neighboring RSFC maps to identify transitions in RSFC across the cortical surface. Consistent edges identified in these gradient maps can be used to generate discrete parcels using the watershed transform (see Supplemental Materials). The parcellation defined by this method demonstrated high reproducibility, such that parcellations derived from two distinct subsets of 42 sessions exhibited considerable overlap (yellow vertices in Figure 1A). The Dice coefficient between these parcellations was 0.87. We further evaluated the internal validity of the parcels generated from the entire dataset using a homogeneity measure defined as the percent of variance explained by the first principal component of the RSFC patterns from all the vertices in each parcel (Gordon et al., 2014b). Mean homogeneity across all parcels was 86.5% ± 7.3% (Figure 1B). This mean homogeneity was significantly greater than that obtained in any of 1000 null model parcellations generated by randomly rotating the original parcellation around the cortical surface (Z-score = 23.1, $p<0.001$; Figure 1C on the left). Notably, homogeneity of the RSFC-derived parcels did not strongly vary by parcel size (red line in Figure 1C), unlike the parcels generated by the null model, which decreased in homogeneity with increasing size (black line), suggesting that the parcellation method can accurately define putative functional areas of variable size. Further, the subject-specific parcellation performed better than our previously-defined group parcellation (Gordon et al., 2014b) evaluated in the same way in the subject data (Z-score = 2.1, $p=.015$) and much better than the AAL atlas (Z-score = −1.3, $p=.907$).

Comparison of subject-specific RSFC-based parcels with task fMRI responses—If parcels defined by RSFC plausibly reflect cortical functional areas, they should correspond to areas defined by other measures of brain functional organization. In the past, we have reported alignment of group-average RSFC-boundaries with both probabilistic cytoarchitectonic maps and group-level task activation maps (Gordon et al., 2014b; Wig et al., 2014b). Although we (necessarily) have no histological measurements in this individual, fMRI responses to a large set of tasks were collected, allowing for both qualitative and quantitative assessments of within-subject correspondence between task and rest.

Correspondence with retinotopy: Putative boundaries between early cortical visual areas V1, V2, and V3 were identified by demarcating reversals in the polar angle map responses to a rotating flickering checkerboard stimulus. Both dorsal and ventral borders of the functionally-defined V1 corresponded well to RSFC-defined parcel edges in both hemispheres (Figure 2; magenta arrows). The boundary between dorsal V2 and dorsal V3 also corresponded to parcel edges in both hemispheres. However, there was no apparent parcel edge corresponding to the boundary between ventral V2 and V3 in either hemisphere. Notably, the RSFC parcellation identified additional boundaries that do not correspond to early visual area boundaries. Some of these boundaries, particularly near the occipital pole,

may relate to local changes in signal quality due to magnetization susceptibility inhomogeneity. Further, more boundaries within the left V1 region were observed than in right V1. This hemispheric asymmetry may reflect weak correlation gradients in the right hemisphere below the edge detection threshold. Of particular interest, however, are the boundaries observed both dorsally and ventrally perpendicular to the long axis of areas V2 and V3. These boundaries reflect relatively large correlation gradients that may relate to distinctions between foveal and peripheral representations of the visual field (cyan arrows) as has been observed in group-averaged data (Buckner et al., 2014; Yeo et al., 2011).

Correspondence with evoked responses to a set of tasks: If RSFC-defined parcels correspond to discrete functional areas, then focal responses to tasks should fall within parcel boundaries. To test this correspondence, we evaluated responses to all contrasts in all tasks and computed the fraction of thresholded responses contained within RSFC-defined parcels (fractional overlap). Raising the statistical threshold (reducing the area of "activation") is expected to systematically increase the fractional overlap (Figure 3B). We found that, averaged across all the task contrasts, this fraction was greater than chance at all t-statistic thresholds (Figure 3B). Further, at an arbitrary task map threshold of t=2.3 (two-tailed ~$p<0.1$), 22 of the 27 task contrasts showed significantly higher overlap with the true parcels than the null model ($p<0.05$; Figure 3C). Activation maps from contrasts in the motion discrimination (3 of 5 contrasts with $p<0.01$), object localizer (10 of 10 contrasts with $p<0.01$), and verbal working memory tasks (1of 3 contrasts with $p<0.01$) corresponded particularly well to RSFC parcels, while responses to the N-back (1 of 6 contrasts with $p<0.01$) and spatial working memory (0 of 3 contrasts with $p<0.01$) tasks corresponded somewhat less well.

Areal network reliability and variability

Evaluation of how much data are needed for brain network estimation—Using the parcel-wise correlation matrix as a practical proxy for overall brain organization, we investigated how much resting state fMRI time is needed to obtain convergent estimates. The results are based on 1000 random samplings of the data acquired over 84 sessions split into two halves. To ensure direct node-to-node comparability, we used the parcels derived from all 84 sessions to define parcel-wise timecourses for both halves of the data (see Figure S1 for system assignment). We observed very high measured correlation (r_M) between the two halves of the data comprising 42 sessions each (r_M =0.99±0.002; Figure 4A). This result defined the upper-limit of correlation network reproducibility to which smaller quantities of data were compared. The average correlation of only one session (9 min) from one half of the data with the full set of sessions from the other half of the data was r_M = .82 ± .04. A steep increase in average similarity (r_M =.92±.01) was observed with three sessions (27 min). Additional improvements were observed up to approximately 10 sessions (90 min; r_M =.97±.005), after which the similarity more slowly approached the asymptotic value of r_M =0.99 (Figure 4B). The graph shown in Figure 4B theoretically is a sigmoid of functional form, $r_M = 1/\sqrt{1+\xi^2}$, where ξ^2 is dominated by a term that is inversely proportional to the quantity of available data (see Figure S2 and the Appendix in Supplemental Materials for an algebraic derivation of the sigmoidal functional form and relevant formulae). This functional

form yields a very good fit to the empirical data and can be used to compute a given similarity to the "true" value. The relevant quantities to compute this model are the measurement error of the correlation between a given parcel pair and the range of correlation values in the set of parcel pairs. Although it is impractical to derive a theoretical reproducibility curve for more complex measurements, e.g., parcellation, limited testing demonstrated that these measurements have lower reproducibility than the correlation matrices with similar quantities of data. For example, the Dice coefficient between a parcellation generated from one session (9 minutes) vs. 42 sessions ~0.27.

Additionally, we found that the correlation matrices calculated from one half of the data converged just as quickly, or even slightly faster, with the other half of the data when sampling shorter epochs over more sessions (e.g., 4.5 minutes from two sessions compared to 9 minutes from one session; Figure 4C, red line). This rapid convergence was also seen even with contiguous segments as short as 1.125 minutes of data sampled from more sessions (i.e. 1.125 minutes from 8 sessions compared to 9 minutes from one session; Figure 4C, blue line).

Comparison of within-subject variability and between-subject variability— Within-subject variability was computed as the standard deviation of the correlation estimated between each parcel-pair across all 84 sessions (using individual system assignment, see Figure S1). Within-subject variability was non-uniformly distributed across systems, with higher variability observed in correlations within and between somato-motor and visual regions (Figure 5A, left). Relatively less variability was observed between fronto-parietal, default mode, ventral attention, and medial parietal regions. The average variability across all correlations for each parcel confirmed the pattern of relatively larger variability in visual, somato-motor, and dorsal attention regions compared to the rest of the brain (Figure 5A, bottom). This pattern is distinct from the pattern of between-subject variability computed over group-defined parcels observed in our 120-subject dataset (Figure 5B; group system assignment defined in (Gordon et al., 2014b)). Between-subject variability was relatively higher in fronto-parietal, cingulo-opercular, attentional, and default mode regions than in visual, auditory and somato-motor regions, as previously reported (Mueller et al., 2013). It should be noted that correlation variability generally was much higher across individuals than across sessions within the individual, particularly in the fronto-parietal, cingulo-opercular, attentional and default regions.

A potential source of inter-session variability in the individual is that on Tuesdays (n = 40 sessions) the subject fasted and abstained from caffeine to prepare for a blood draw, while on Thursdays (n = 32 sessions) the subject was fed and caffeinated. We observed differences in correlation strengths between Tuesday and Thursday, with increased correlations within and between somato-motor and extrastriate visual regions (Vis 2) on Thursdays relative to Tuesdays (see Figure S3A; further detailed in Poldrack et al (in revision)). Although these effects of day likely account for some of the observed variability reported above, correlation variability was still relatively higher in visual and somato-motor regions in Tuesday or Thursday acquisitions considered separately (Figure S3B).

Vertex-wise system estimation

Comparison of individual system definition to group system definition—

Systems were defined using Infomap-based community detection in the individual and compared to similar results obtained in the group (Figure 6). The systems have been color-coded using the same scheme where possible. Most systems were grossly topologically similar in the individual and the group including: default mode, visual, dorsal attention, ventral attention, fronto-parietal, cingulo-opercular, salience, auditory, somato-motor, medial parietal, and parieto-occipital systems. Furthermore, this commonality extended to detailed features of systems. For example, smaller regions of the fronto-parietal system in the anterior insula and in dorsal medial prefrontal cortex appear in both the individual and the group (magenta circles). The overall Dice coefficient between the individual and group consensus maps is 0.52.

By contrast, some features of the system maps were markedly different between the individual and the group. The Infomap algorithm did not define lateral somato-motor (orange arrows) or medial temporal systems in the individual, as were found in the group. On the other hand, the individual had a clearly defined primary visual system that was not seen in the group (olive arrows). Prior reports (McAvoy et al., 2008; Xu et al., 2014) suggest that the presence of a primary visual system and the lack of the ventral somato-motor system might relate to a difference in eye state between the individual (eyes closed) and group (eyes open) data. Indeed, an additional 100 minutes of eyes open data collected in the individual as part of a validation dataset confirmed that the effect of eye state is localized primarily to occipital cortex and regions adjacent to the pre- and post-central gyri, identified as visual, somato-motor and dorsal attention regions in this individual (see Figure S4).

Several additional systems were also observed in the primary subject that were not present in the group consensus map. Unlike the primary visual system, which was seen at every tested edge density, these unknown systems were only observed at lower edge densities (see Figure S5), indicating that they were less readily separable from other systems and therefore may be of dubious status. One further observation worth noting is that the group consensus map includes a region in the lateral occipital-temporal cortex (between the default mode and visual systems) without system assignment; in the individual, this same region showed unambiguous system affiliation (Figure 6, green squares).

Fine-grained features in the individual's system map were present across many edge densities. Although we cannot specifically address all of these features, we highlight the pattern of correlation in two adjacent regions of the lateral frontal cortex in the individual relative to the group (Figure 7). In the individual, these two adjacent regions showed starkly divergent patterns of functional connectivity: the Infomap algorithm identified the more anterior region as part of the cingulo-opercular system and the more posterior region as part of the fronto-parietal system. In contrast, the same two adjacent regions in the group showed only local differences in functional connectivity and essentially no long-range differences. Furthermore, a direct comparison of RSFC maps, vertex by vertex, between the individual and the group confirmed a group-individual discrepancy in the example lateral frontal region of Figure 7, as well as many other focal regions with distinct patterns of RSFC (Figure S6A, top row). To ensure that the observed differences between the primary subject and the group

were not related to differences between scanners and fMRI sequence parameters, an additional validation dataset (100 minutes eyes-closed rest) was collected on the primary subject at the Washington University site with the same fMRI sequence as the group data. The focal individual vs. group differences were replicated in the validation dataset (Figure S6A, second row).

To evaluate whether such focal differences are unique to this particular highly-sampled individual or a more general feature of individual brain organization, we collected an extensive dataset (10 runs of 30-minutes) on an additional subject ('secondary subject'). The Infomap-based community detection result at several edge densities are reported for this individual and compared to the group system map in Figure S7. This second individual also exhibited many of the same systems as the group data. As this individual's data were collected with eyes open, it should be noted that, unlike the primary subject, this individual did not have a separate primary visual system but did have a separate ventral somatomotor system (Figure S7, middle rows). Further, focal differences between this second individual and the group were observed primarily in frontal and parietal regions (Figure S7, bottom row), as in the primary subject, although the exact locations were different. Together, these observations illustrate the existence of idiosyncratic topological features in functional brain organization specific to each individual.

Discussion

We present a description of the functional organization of a single human brain, based on functional MRI measurements repeatedly sampled over more than a year. Resting-state correlation-based functional organization was highly reproducible in this individual. The areal parcellation derived from resting state data corresponded with aspects of retinotopically defined visual areas and fMRI responses to task paradigms in the same individual. Across-session variability in RSFC was greater in visual, somato-motor, and dorsal attention regions relative to other regions, though considerably less overall than between-subject variability. Finally, we found that functional systems are largely similar in the individual and in the group, but that some features in the individual were topologically distinct.

Subject-specific RSFC-based parcels are reproducible and show internal validity

RSFC-based subject-specific parcellation was reproducible across subsets of data and internally valid according to the criteria defined in (Gordon et al., 2014b). In particular, the subject-specific parcellation exhibited high parcel-wise homogeneity, and the whole parcellation was significantly more homogenous than a null model. This result suggests that, as a whole, the parcellation effectively delineates functionally homogenous cortical areas in this individual, and therefore is likely to represent a neurobiologically meaningful basis for brain network analyses (Power et al., 2011; Smith et al., 2011; Wig et al., 2011).

The final parcellation included 616 parcels across both cortical hemispheres. This figure is somewhat greater than the 150-200 human cortical areas per hemisphere estimated by (Van Essen et al., 2012), and also greater than the 333 parcels previously identified in group-average data (Gordon et al., 2014b). RSFC-based parcellation is capable of finding

functional subdivisions within traditionally defined cortical areas, e.g., putative distinctions between tongue, hand, and foot representations within Brodmann areas 3 and 4 (Gordon et al., 2014b). Here, even finer delineation of specific functional subdivisions was possible, most likely because imperfect registration of functional systems across individuals was avoided. Our experience indicates that the precise number of parcels and exact position of the parcel boundaries may vary with processing choices (e.g., smoothing, edge retention threshold), but the general shape and position of parcels does not significantly change. Thus, the current parcel set should be viewed as a current best estimate for this subject.

Subject-specific RSFC-based parcels correspond to task-evoked responses

Correspondence between group-level resting state correlation organization and task co-activation patterns has been amply documented (Cordes et al., 2000; Power et al., 2011; Smith et al., 2009; Wig et al., 2014a). However, subject-specific task-rest correspondence has been more difficult to demonstrate. (Blumensath et al., 2013) have reported that RSFC measurements track task responses in individuals. Here, with the advantage of a much larger dataset, we observed a significant correspondence between subject-specific RSFC-defined parcels and task evoked responses. The V1/V2 boundary defined by retinotopic mapping clearly corresponded to RSFC-based parcel edges. This result replicates, in an individual, our previous observations at the group-level of a correspondence between RSFC-derived parcels and cytoarchitectonic boundaries between probabilistic areas 17 and 18 (Gordon et al., 2014b; Wig et al., 2014b). Areas V2 and V3 also showed correspondence with RSFC-defined parcel edges, albeit less consistently and only dorsally. As noted above, RSFC-defined parcels need not correspond exactly with classically defined cortical areas. Indeed, we observed RSFC-defined parcel edges in this individual that may correspond to foveal vs. peripheral representations of the visual field (Buckner et al., 2014).

Similarly, some task responses corresponded better to the RSFC-based parcellation than others. In particular, the object localizer, verbal working memory, and motion discrimination tasks produced activation patterns that better aligned with parcels than the N-back and spatial working memory tasks. Although the reasons for this observation are uncertain, one possibility is that some task contrasts may be less process-specific than others, leading to a loss of specificity of evoked responses across neighboring functional areas. Reduced specificity may reflect multiple distinct processes invoked in a given task condition or alternate cognitive strategies used in different task sessions. Of course, the set of tasks used for this study does not represent the universe of tasks needed to delineate the full complement of cortical functional areas. However, the presently demonstrated task-rest correspondence so far observed in this dataset validates the principle that subject-specific parcellations can inform future network analyses.

Measures of individual functional brain organization converge with sufficient data

We found that 9 minutes of data generated respectable reproducibility of correlation network estimates with respect to the “true” correlation matrix (average $r_M = 0.82$). However, systematically varying the quantity of data revealed greatly improved precision of correlation matrix estimates as the quantity of data increased from 9 minutes to 27 minutes, and beyond, in accordance with theory taking into account measurement error and the range

of values in the correlation matrix (see Supplemental Materials). This result is consistent with recent reports (Anderson et al., 2011; Birn et al., 2013; Hacker et al., 2013). Thus, 5-10 minutes of data, as commonly collected in many resting-state studies, may not capture a precise representation of stationary functional connectivity features of individual subjects. Further, it should be noted that the presented reproducibility values correspond to the relatively robust measure of correlation estimates from mean parcel timecourses. Achieving similar levels of reproducibility for more fine-grained measures of brain organization (e.g., parcellation) may be expected to require extended per-subject datasets, as collected here.

It is possible to effectively measure individual brain organization with multiple scans of shorter length (e.g., 5 minutes), provided that a sufficient number of scans are acquired. This observation may have implications for study designs in populations in which longer scans may be difficult to obtain (e.g., children). Functional connectivity estimates in the primary subject converged at approximately 100 minutes of total scanning time. Although acquiring this much data in individuals is not feasible in many contexts, 100 minutes could be seen as aspirational for those interested in comprehensively characterizing single-subject features of RSFC, which may be desirable when investigating the network organization of special or rare individuals.

Sources of within-subject variability in functional connectivity are different than sources of between-subject variability

Within-subject variability in RSFC was not uniformly distributed across the cortex. In particular, visual, somato-motor and some dorsal attention regions were more variable than other regions of the brain. In stark contrast, between-subject variability was relatively lower in somato-motor and visual regions than in default mode, attentional, and control network regions. This result expands on previous findings reported by Mueller et al (2013) and suggests that sources of within-subject variability vs. between-subject variability are distinct. Specifically, the large between-subject variability of correlation estimates in frontal and parietal regions may reflect inter-individual variability in cortical folding patterns (Hill et al., 2010), variable localization of functional areas with respect to sulcal anatomy (Frost et al., 2012), and/or variable system topologies (as discussed below). These factors could lead to misalignment of cortical regions thereby increasing apparent correlation variability as assessed by the group-averaged parcellation used here. However, anatomical variability cannot explain the presently observed pattern of within-subject correlation variability. Other than measurement error (the dominant source of variance according to the model defined in the Appendix), there are several known biological sources of within-subject variability. In particular, slow biological processes such as diurnal rhythms have been shown to significantly modify spontaneous BOLD activity (Hodkinson et al., 2014; Shannon et al., 2013). In the present case, however, the vast majority of scans were collected at the same time of day (7:30 AM). More generally, any intra-day BOLD fluctuations longer than ten minutes are unobservable with this data. Alternatively, numerous studies have demonstrated specific effects of different cognitive and behavioral contexts on resting-state activity (e.g., (Gordon et al., 2014a; Lewis et al., 2009; Tambini et al., 2010). Such cognitive/behavioral contexts could not be entirely controlled from session to session and therefore may have contributed to cross-session variability. A third possible source of variability is metabolic

state (i.e. fed or fasted, caffeinated or uncaffeinated) – addressed in more detail below. Other unidentified sources of RSFC variability are likely to exist (e.g., fluctuating hormones, mood, gene expression, longitudinal seasonal or aging-related changes, etc.), the discovery of which is one of the explicit objectives of acquiring this dataset (described in Poldrack et al (in revision)), but discussion of which is out of scope in the present report. Although sampling error is the primary source of variability in functional connectivity estimates, those additional sources of variability contribute to the necessity of acquiring large quantities of data to obtain stable measurements of brain organization.

Systematic effects attributable to fasted/uncaffeinated (Tuesdays) vs. fed/caffeinated (Thursdays) states were observed in extrastriate visual regions and somato-motor regions. This result is consistent with the previous finding that caffeine reduces measured RSFC in motor cortex (Rack-Gomer et al., 2009). Although fasting/caffeination accounts for some of the increased within-subject variability described above, within-subject variability was still relatively higher in somato-motor and particularly visual regions in Tuesday and Thursday acquisitions considered separately. This residual variability most likely reflects variable arousal across sessions, as (Tagliazucchi et al., 2014) have recently reported increased BOLD variance in somato-motor and visual regions during light sleep relative to waking. Unfortunately, we did not acquire simultaneous EEG-fMRI to confirm this possibility. However, Poldrack et al (in revision) found that the effect of Tuesday vs. Thursday differences on connectivity within these networks was partially attributable to fatigue measured immediately after the scan. In any case, multiple sources of variability potentially affect day-to-day correlation estimates in an individual. Hence, a comprehensive picture of functional organization may not be achievable in a single session. On the other hand, inter-session variability is dwarfed by between-subject variability. Hence, inter-individual variability is the dominant confound in studies of group-level differences.

Individual functional brain organization shows similar system definition as group but also exhibits distinct functional topology

Almost all of the RSFC systems and their topological relations identified in the individual were also found in the group. Several spatial motifs in the adjacencies of group-average systems observed in prior work (Power et al., 2011) are also present in the individual, including the default/salience/cingulo-opercular and the somato-motor/dorsal-attention/fronto-parietal interfaces. The presence of these topological motifs (salience and dorsal-attention) in both individuals provides further evidence that they are not the result of intermixed signals generated by averaging, a concern posed in the previous work. On the other hand, the frontal-parietal-temporal subgraph found in that work, interposed between default and fronto-parietal systems (light blue in Power 2011), does not have an analogous system in these individuals. Additional highly-sampled subjects will be needed to confirm whether this is a general observation of individual functional brain organization. The two most notable differences between the individual and the group Infomap results are the absence in the individual of the lateral somato-motor system and the presence of an additional system in primary visual cortex. These differences are consistent with previously described effects of eyes closed (individual) vs. eyes open (group) resting state data. The eyes closed state has been shown to increase spontaneous BOLD fluctuations in visual and

somato-motor regions (McAvoy et al., 2008), and enhance visual:somato-motor correlations (Xu et al., 2014). Direct comparison of eyes closed and eyes open data collected in our validation dataset confirm that eye state has localized effects in visual, somato-motor, and adjacent regions (see Figure S4). These differences in RSFC between eye states likely account for several of the system-level differences between the individual and the group. However, eye state does not explain the more focal differences discussed below.

Figure 7 highlights a detailed topological feature that is notably different in the primary subject as compared to the group. This and other topological differences between the primary subject and the group apparent in Figure 6 (e.g., fronto-parietal system patches in the right medial prefrontal and posterior cingulate cortex; ventral attention and default mode patches in left middle frontal gyrus) and between the second subject and the group (see arrows in Figure S7) indicate clear individual differences in RSFC (see Figure S6A and S7 bottom row). The group data were geodesically registered on the surface based on macro-anatomic sulcal and gyral features; this registration represents the current state of the art, but it does not achieve a true area-to-area registration (Frost et al., 2012). Thus, group-level averaging of RSFC patterns necessarily blurs over functionally variable regions, creating the appearance of reduced topological complexity. Such blurring may explain the inability to assign a system identity to the blank region in lateral occipital-temporal cortex in the group result, where there are clear system identities in each individual (Figure 6).

The observation of distinct topological features in individuals raises an interesting possibility concerning brain organization. If we assume that brain systems are composed of functionally related cortical areas, and that cortical areas are unlikely to be translated over large distances across the cortical surface, then the present evidence suggests that some cortical areas are connected to different systems in different individuals. In other words, some cortical areas may be functionally variable across individuals in their general relationships with other brain areas. Verification of this possibility will require collecting similarly massive data sets on more than just two individuals.

Further, from a methodological standpoint, this observation may have important implications for techniques that attempt to incorporate functional responses into a registration algorithm. Registration strategies have been proposed to improve alignment between subjects taking into account functional variability (Robinson et al., 2014; Sabuncu et al., 2010). However, these schemes rely on having sufficient data in each individual to accurately estimate individual functional topography. Further, such registrations can only align topologically consistent features. If, however, individuals exhibit true topological differences in functional organization, e.g., different numbers of disjoint regions within a given system or different systems attributed to a given cortical area, then complete subject-to-subject alignment in brain space may be not be achievable. Again, confirmation of this possibility will require reliable characterization of the functional brain organization of multiple highly sampled individuals.

Conclusion—This dataset was originally collected in order to comprehensively and longitudinally phenotype a single human with the objective of relating dynamics in brain function to other biological and environmental variables. Successful attribution of such

relationships requires accurate description of the individual's functional brain organization. We have used this rich dataset to characterize the functional brain organization of the individual at multiple scales and to determine how it varies over repeated sessions. We observed broad similarity as well as intriguing specific differences with group data. Any study reporting observations in one or two subjects has necessarily limited generality. Specific features described in these individuals could be explained as idiosyncratic (perhaps reflecting willingness to undergo such extensive self-experimentation). Therefore, we do not assign specific meaning to the detailed features observed here. However, we believe that the reliable presence of these detailed features in each individual must motivate further studies of this type. These studies may inform the understanding of individual differences in brain function and, potentially, cognition. In particular, we believe that the subject-specific approach outlined here may be essential for understanding the functional brain organization of unique or rare subjects (e.g., cognitive savants, rare disease populations, or brain-injured subjects like HM). Indeed, the present results provide a foundation for analyses of brain-behavior relationships that respect the specific anatomic and functional contours of a particular individual's brain.

Experimental Procedures

Highly-Sampled Subject Characteristics

The primary subject (author RP) is a right-handed Caucasian male, aged 45 years-old at the onset of the study. RP is generally healthy apart from mild plaque psoriasis. Prior to initiation of the pilot period, RP had a physical examination with full blood workup revealing not significant findings. RP has a history of anxiety disorder, but no other neuropsychiatric disorders. An additional extensive dataset was acquired in a right-handed, 34-year-old Caucasian male (author ND). ND was scanned at Washington University.

Primary Subject Data Acquisition

The primary data in the primary subject were collected over the course of 532 days. Scans were performed at fixed times of day: Mondays at 5 pm, and Tuesdays and Thursdays at 7:30 am. Imaging was performed with a Siemens Skyra 3T MRI scanner using a 32-channel coil and a multi-band EPI (MBEPI) sequence [TR = 1.16 seconds; 2.4 mm isotropic voxels] (Moeller et al., 2010). Resting-state fMRI was acquired in the eyes-closed condition. 84 sessions were used in the present analyses. The first minute of each resting state scan was discarded to exclude transient fMRI responses evoked by the scan start and noise-cancelling headphones. A series of tasks also were collected at various times during the scanning period (n=51 task fMRI sessions) including N-back, motion discrimination, object presentation, verbal working memory, spatial working memory and retinotopy. See Supplemental Materials for acquisition and task fMRI details.

To control for site/scanner differences in comparisons of the primary subject vs. the group, a validation dataset was collected at Washington University using the same fMRI sequence as in the 120-subject group. This dataset comprised ten 10-minute runs of eyes closed resting state data and ten 10-minute runs of eyes open (and fixated) resting state data. All data for

this subject are available at the OpenfMRI repository (http://openfmri.org/dataset/ds000031). See Table S1 for comparison of acquisition parameters for all collected datasets.

Secondary Subject Data Acquisition

Subject ND was scanned at Washington University using a 3T TIM TRIO scanner equipped with 12-channel coil and a (single-band) EPI sequence [TR = 2.2seconds; 4-mm isotropic voxels]. Ten 30-minute eyes open resting-state runs with passive fixation (total 300 minutes) were acquired over 10 days. Subjects ND and RP were analyzed using the same procedures.

Group Data Acquisition and Processing

Group comparisons were based on an extant dataset of 120 subjects studied at Washington University. These subjects have been characterized in great detail elsewhere (Gordon et al., 2014b; Power et al., 2014; Wig et al., 2014b). All subjects were healthy young adults (60 females, mean age = 25 years, age range = 19-32 years), native speakers of English and right-handed. Subjects were screened to exclude a history of neurological or psychiatric diagnoses. Informed consent was obtained in all subjects. Resting state fMRI with eyes open and fixated on a crosshair was acquired using a 3T TIM TRIO system equipped with a 12-channel coil and a (single-band) EPI sequence [TR = 2.5 seconds; 4 mm isotropic voxels]. The group data were processed as described in (Gordon et al., 2014b). Processing of the group data did not include field distortion correction, as field maps were not acquired in all subjects.

fMRI Preprocessing

Functional data were preprocessed to reduce artifact and to maximize cross-session registration. Data were resampled to 3-mm isotropic atlas space including mean field distortion correction and motion correction in a single interpolation step. Additional RSFC preprocessing followed the procedures described in (Power et al., 2014), including motion scrubbing; white matter, CSF, and global signal regression; and temporal filtering. See Supplemental Materials for details of distortion correction, fMRI preprocessing, and RSFC preprocessing.

Surface processing and CIFTI generation

Surface extraction and sampling of functional data to the brain surface followed procedures similar to those previously described in (Glasser et al., 2013). Processed RSFC data were sampled to subject-specific FreeSurfer generated surfaces and registered to a common fs-LR space (Van Essen et al., 2012). The surface data were combined with volumetric subcortical data into CIFTI format using Connectome Workbench. See Supplemental Materials for more details.

Parcellation Validation

The single-subject parcellation was generated following the procedures described in detail in (Gordon et al., 2014b) and (Wig et al., 2014b); details in supplementary methods). Parcel homogeneity was evaluated as the percent of variance explained by the first eigenvector computed from a principal component analysis (PCA) of the RSFC patterns from all vertices

in the parcel (Gordon et al., 2014b). The overall homogeneity of the parcellation was compared to a null model consisting of the homogeneity computed from 1000 random rotations of the parcellation on the surface. The validated parcellation forms the basis for many of the analyses reported here.

Task vs. Rest comparison

Under the assumption that task activations should correspond to RSFC-defined parcels rather than parcel boundaries, we measured the fraction of task-activated vertices that fell within the RSFC-defined parcels. A measured fraction greater than the expected fraction from random placement of non-edge parcel vertices (~70% of the cortical surface) would indicate correspondence between the parcellation and the task activations. However, to account for the known spatial autocorrelation of BOLD fMRI data and the topological dependencies of the parcel detection procedure, i.e. the fact that boundary vertices will by definition neighbor other boundary vertices, we developed a further null model to test for correspondence between task and rest. As in the parcellation homogeneity validation (Gordon et al., 2014b), we randomly rotated the true parcellation along the cortical surface 1000 times. We then computed the fraction of task-activated regions that fell within the randomly rotated parcels. Regions with particularly low SNR as measured by mean BOLD fMRI across all sessions (mode 1000-normalized voxel value < 800) were ignored. From this null distribution, we derived a non-parametric statistic of significance indicating how well each task activation corresponded to the true parcellation.

Evaluating parcel-wise correlation estimate convergence

We used the parcels derived from all 84 sessions to extract parcel-wise resting state timecourses from each session. Cross-correlation of these timecourses was computed to define parcel-by-parcel correlation matrices representing the areal-level brain network. A split-half procedure was used to evaluate how much data were needed to obtain convergent estimates of this parcel correlation matrix. The 84 sessions were repeatedly split into two randomly selected subsets of sessions. A correlation matrix was computed using concatenated timecourses from all the sessions of one subset (n = 42; 380 minutes of data). The similarity between this ‘true’ correlation matrix and the correlation matrix derived from varying amounts of the remaining subset of sessions was computed using Pearson's correlation (r_M , measured correlation matrix similarity). To evaluate the effect of session variability over and above pure scan time we also computed the correlation matrix similarity to matrices generated by contiguous sampling of the same number of frames but from a larger number of sessions (e.g., 9 minutes from 1 session compared to 9 minutes from 4.5 minutes of 2 sessions).

System Assignment

The system organization of the vertex/voxel-wise and parcel-wise graphs were computed using the Infomap algorithm (Rosvall et al., 2008), following (Power et al., 2011), where graph nodes represent either cortical surface vertices and sub-cortical/cerebellar voxels, or parcel-based regions of interest. A cross-correlation matrix of the concatenated time courses from all sessions defined the edges between nodes. For parcels, these time courses were computed by averaging timecourses across all vertices within the parcel. Vertex connections

within 10 mm of each other (or 30 mm between parcel centers) were removed from consideration to avoid correlations attributable to spatial smoothing. Geodesic distance was used for surface connections and Euclidean distance for sub-cortical and interhemispheric connections. System assignments were computed at a range of edge densities (0.05% to 5%). Systems with 400 or fewer vertices or voxels (or 8 or fewer parcels) were considered unassigned and removed from further consideration.

The Infomap procedure was also applied to the group dataset. The systems generated in this way followed very closely the results reported in (Power et al., 2011), with the refinement of improved cross-subject alignment attributable to surface registration. A ‘consensus’ assignment was derived by collapsing across thresholds as described in (Gordon et al., 2014b), giving each node the assignment it has at the sparsest possible threshold at which it was successfully assigned. The subject's Infomap-derived systems were matched to the group consensus systems by computing the average geodesic distance between the vertices of each system in the individual system map and the closest vertex of each system in the group system map, and vice versa. System-to-system assignment was determined by minimizing this distance metric across all systems using the Hungarian algorithm (Bourgeois, 1971). The edge density with the least overall cost to match with the group consensus map formed the basis for the individual consensus map. The present network assignment procedure is not meant to provide an exhaustive description of network organization and may not capture non-hierarchical network features. We also do not report subcortical or cerebellar Infomap results as network assignment for these regions typically requires specialized analysis procedures (see e.g. (Buckner et al., 2011; Greene et al., 2014; Zhang et al., 2008).

Supplementary Material

Refer to Web version on PubMed Central for supplementary material.

Acknowledgements

This work was supported by MH100872 (TOL), NS61144 (SEP), NS26424 (SEP), P30NS048056 (AZS), a McDonnell Foundation Collaborative Activity award (SEP), Hope Center for Neurological Disorders Pilot Award (BLS), Intellectual and Developmental Disabilities Research Center at Washington University (NIH/NICHDP30 HD062171), Mallinckrodt Institute of Radiology Pilot Grant (NUFD), Child Neurology Foundation Scientific Research Award (NUFD), WU Child Health Research Center K12-HD076224 (Alan Schwartz), McDonnell Center for Systems Neuroscience New Resource Proposal (NUFD), NS088590 (NUFD), Dart NeuroScience LLC (KBM), MH091657 (Van Essen), and the Texas Emerging Technology Fund (D. Johnston, PI). We thank Alex Huk for facilitating data collection and Jonathan Power for helpful comments on the manuscript.

References

Anderson JS, Ferguson MA, Lopez-Larson M, Yurgelun-Todd D. Reproducibility of single-subject functional connectivity measurements. AJNR Am J Neuroradiol. 2011; 32(3):548–555. [PubMed: 21273356]

Birn RM, Molloy EK, Patriat R, Parker T, Meier TB, Kirk GR, Nair VA, Meyerand ME, Prabhakaran V. The effect of scan length on the reliability of resting-state fMRI connectivity estimates. Neuroimage. 2013; 83:550–558. [PubMed: 23747458]

Biswal B, Yetkin FZ, Haughton VM, Hyde JS. Functional connectivity in the motor cortex of resting human brain using echo-planar MRI. Magn Reson Med. 1995; 34(4):537–541. [PubMed: 8524021]

Blumensath T, Jbabdi S, Glasser MF, Van Essen DC, Ugurbil K, Behrens TE, Smith SM. Spatially constrained hierarchical parcellation of the brain with resting-state fMRI. Neuroimage. 2013; 76:313–324. [PubMed: 23523803]

Bourgeois FL, JC. An extension of the Munkres algorithm for the assignment problem to rectangular matrices. Communications of the Association for Computing Machinery. 1971; 14(12):802–804.

Buckner RL, Krienen FM, Castellanos A, Diaz JC, Yeo BT. The organization of the human cerebellum estimated by intrinsic functional connectivity. J Neurophysiol. 2011; 106(5):2322–2345. [PubMed: 21795627]

Buckner RL, Yeo BT. Borders, map clusters, and supra-areal organization in visual cortex. Neuroimage. 2014; 93(Pt 2):292–297. [PubMed: 24374078]

Choi EY, Yeo BT, Buckner RL. The organization of the human striatum estimated by intrinsic functional connectivity. J Neurophysiol. 2012; 108(8):2242–2263. [PubMed: 22832566]

Churchland PS, Sejnowski TJ. Perspectives on cognitive neuroscience. Science. 1988; 242(4879):741–745. [PubMed: 3055294]

Cohen AL, Fair DA, Dosenbach NU, Miezin FM, Dierker D, Van Essen DC, Schlaggar BL, Petersen SE. Defining functional areas in individual human brains using resting functional connectivity MRI. Neuroimage. 2008; 41(1):45–57. [PubMed: 18367410]

Cordes D, Haughton VM, Arfanakis K, Wendt GJ, Turski PA, Moritz CH, Quigley MA, Meyerand ME. Mapping functionally related regions of brain with functional connectivity MR imaging. AJNR Am J Neuroradiol. 2000; 21(9):1636–1644. [PubMed: 11039342]

Damoiseaux JS, Rombouts SA, Barkhof F, Scheltens P, Stam CJ, Smith SM, Beckmann CF. Consistent resting-state networks across healthy subjects. Proc Natl Acad Sci U S A. 2006; 103(37):13848–13853. [PubMed: 16945915]

Devlin JT, Poldrack RA. In praise of tedious anatomy. Neuroimage. 2007; 37(4):1033–1041. discussion 1050-1038. [PubMed: 17870621]

Dosenbach NU, Fair DA, Miezin FM, Cohen AL, Wenger KK, Dosenbach RA, Fox MD, Snyder AZ, Vincent JL, Raichle ME, et al. Distinct brain networks for adaptive and stable task control in humans. Proc Natl Acad Sci U S A. 2007; 104(26):11073–11078. [PubMed: 17576922]

Doucet G, Naveau M, Petit L, Delcroix N, Zago L, Crivello F, Jobard G, Tzourio-Mazoyer N, Mazoyer B, Mellet E, et al. Brain activity at rest: a multiscale hierarchical functional organization. J Neurophysiol. 2011; 105(6):2753–2763. [PubMed: 21430278]

Felleman DJ, Van Essen DC. Distributed hierarchical processing in the primate cerebral cortex. Cereb Cortex. 1991; 1(1):1–47. [PubMed: 1822724]

Fischl B, Sereno MI, Dale AM. Cortical surface-based analysis. II: Inflation, flattening, and a surface-based coordinate system. Neuroimage. 1999; 9(2):195–207. [PubMed: 9931269]

Fox PT, Perlmutter JS, Raichle ME. A stereotactic method of anatomical localization for positron emission tomography. J Comput Assist Tomogr. 1985; 9(1):141–153. [PubMed: 3881487]

Frost MA, Goebel R. Measuring structural-functional correspondence: spatial variability of specialised brain regions after macro-anatomical alignment. Neuroimage. 2012; 59(2):1369–1381. [PubMed: 21875671]

Glasser MF, Sotiropoulos SN, Wilson JA, Coalson TS, Fischl B, Andersson JL, Xu J, Jbabdi S, Webster M, Polimeni JR, et al. The minimal preprocessing pipelines for the Human Connectome Project. Neuroimage. 2013; 80:105–124. [PubMed: 23668970]

Gordon EM, Breeden AL, Bean SE, Vaidya CJ. Working memory-related changes in functional connectivity persist beyond task disengagement. Hum Brain Mapp. 2014a; 35(3):1004–1017. [PubMed: 23281202]

Gordon EM, Laumann TO, Adeyemo B, Huckins JF, Kelley WM, Petersen SE. Generation and Evaluation of a Cortical Area Parcellation from Resting-State Correlations. Cereb Cortex. 2014b

Greene DJ, Laumann TO, Dubis JW, Ihnen SK, Neta M, Power JD, Pruett JR Jr. Black KJ, Schlaggar BL. Developmental changes in the organization of functional connections between the basal ganglia and cerebral cortex. J Neurosci. 2014; 34(17):5842–5854. [PubMed: 24760844]

Hacker CD, Laumann TO, Szrama NP, Baldassarre A, Snyder AZ, Leuthardt EC, Corbetta M. Resting state network estimation in individual subjects. Neuroimage. 2013; 82:616–633. [PubMed: 23735260]

Hill J, Dierker D, Neil J, Inder T, Knutsen A, Harwell J, Coalson T, Van Essen D. A surface-based analysis of hemispheric asymmetries and folding of cerebral cortex in term-born human infants. J Neurosci. 2010; 30(6):2268–2276. [PubMed: 20147553]

Hodkinson DJ, O'Daly O, Zunszain PA, Pariante CM, Lazurenko V, Zelaya FO, Howard MA, Williams SC. Circadian and homeostatic modulation of functional connectivity and regional cerebral blood flow in humans under normal entrained conditions. J Cereb Blood Flow Metab. 2014; 34(9):1493–1499. [PubMed: 24938404]

Lewis CM, Baldassarre A, Committeri G, Romani GL, Corbetta M. Learning sculpts the spontaneous activity of the resting human brain. Proc Natl Acad Sci U S A. 2009; 106(41):17558–17563. [PubMed: 19805061]

McAvoy M, Larson-Prior L, Nolan TS, Vaishnavi SN, Raichle ME, d'Avossa G. Resting states affect spontaneous BOLD oscillations in sensory and paralimbic cortex. J Neurophysiol. 2008; 100(2): 922–931. [PubMed: 18509068]

Moeller S, Yacoub E, Olman CA, Auerbach E, Strupp J, Harel N, Ugurbil K. Multiband multislice GE-EPI at 7 tesla, with 16-fold acceleration using partial parallel imaging with application to high spatial and temporal whole-brain fMRI. Magn Reson Med. 2010; 63(5):1144–1153. [PubMed: 20432285]

Mueller S, Wang D, Fox MD, Yeo BT, Sepulcre J, Sabuncu MR, Shafee R, Lu J, Liu H. Individual variability in functional connectivity architecture of the human brain. Neuron. 2013; 77(3):586–595. [PubMed: 23395382]

Power JD, Cohen AL, Nelson SM, Wig GS, Barnes KA, Church JA, Vogel AC, Laumann TO, Miezin FM, Schlaggar BL, et al. Functional network organization of the human brain. Neuron. 2011; 72(4):665–678. [PubMed: 22099467]

Power JD, Mitra A, Laumann TO, Snyder AZ, Schlaggar BL, Petersen SE. Methods to detect, characterize, and remove motion artifact in resting state fMRI. Neuroimage. 2014; 84:320–341. [PubMed: 23994314]

Rack-Gomer AL, Liau J, Liu TT. Caffeine reduces resting-state BOLD functional connectivity in the motor cortex. Neuroimage. 2009; 46(1):56–63. [PubMed: 19457356]

Robinson EC, Jbabdi S, Glasser MF, Andersson J, Burgess GC, Harms MP, Smith SM, Van Essen DC, Jenkinson M. MSM: a new flexible framework for Multimodal Surface Matching. Neuroimage. 2014; 100:414–426. [PubMed: 24939340]

Rosvall M, Bergstrom CT. Maps of random walks on complex networks reveal community structure. Proc Natl Acad Sci U S A. 2008; 105(4):1118–1123. [PubMed: 18216267]

Sabuncu MR, Singer BD, Conroy B, Bryan RE, Ramadge PJ, Haxby JV. Function-based intersubject alignment of human cortical anatomy. Cereb Cortex. 2010; 20(1):130–140. [PubMed: 19420007]

Shannon BJ, Dosenbach RA, Su Y, Vlassenko AG, Larson-Prior LJ, Nolan TS, Snyder AZ, Raichle ME. Morning-evening variation in human brain metabolism and memory circuits. J Neurophysiol. 2013; 109(5):1444–1456. [PubMed: 23197455]

Shehzad Z, Kelly AM, Reiss PT, Gee DG, Gotimer K, Uddin LQ, Lee SH, Margulies DS, Roy AK, Biswal BB, et al. The resting brain: unconstrained yet reliable. Cereb Cortex. 2009; 19(10):2209–2229. [PubMed: 19221144]

Smith SM, Fox PT, Miller KL, Glahn DC, Fox PM, Mackay CE, Filippini N, Watkins KE, Toro R, Laird AR, et al. Correspondence of the brain's functional architecture during activation and rest. Proc Natl Acad Sci U S A. 2009; 106(31):13040–13045. [PubMed: 19620724]

Smith SM, Miller KL, Salimi-Khorshidi G, Webster M, Beckmann CF, Nichols TE, Ramsey JD, Woolrich MW. Network modelling methods for FMRI. Neuroimage. 2011; 54(2):875–891. [PubMed: 20817103]

Tagliazucchi E, Laufs H. Decoding wakefulness levels from typical fMRI resting-state data reveals reliable drifts between wakefulness and sleep. Neuron. 2014; 82(3):695–708. [PubMed: 24811386]

Tambini A, Ketz N, Davachi L. Enhanced brain correlations during rest are related to memory for recent experiences. Neuron. 2010; 65(2):280–290. [PubMed: 20152133]

Van Dijk KR, Hedden T, Venkataraman A, Evans KC, Lazar SW, Buckner RL. Intrinsic functional connectivity as a tool for human connectomics: theory, properties, and optimization. J Neurophysiol. 2010; 103(1):297–321. [PubMed: 19889849]

Van Essen DC, Dierker D. On navigating the human cerebral cortex: Response to 'in praise of tedious anatomy'. Neuroimage. 2007; 37(4):1050–1054. [PubMed: 17766148]

Van Essen DC, Glasser MF, Dierker DL, Harwell J, Coalson T. Parcellations and hemispheric asymmetries of human cerebral cortex analyzed on surface-based atlases. Cereb Cortex. 2012; 22(10):2241–2262. [PubMed: 22047963]

Wig GS, Laumann TO, Cohen AL, Power JD, Nelson SM, Glasser MF, Miezin FM, Snyder AZ, Schlaggar BL, Petersen SE. Parcellating an individual subject's cortical and subcortical brain structures using snowball sampling of resting-state correlations. Cereb Cortex. 2014a; 24(8):2036–2054. [PubMed: 23476025]

Wig GS, Laumann TO, Petersen SE. An approach for parcellating human cortical areas using resting-state correlations. Neuroimage. 2014b; 93(Pt 2):276–291. [PubMed: 23876247]

Wig GS, Schlaggar BL, Petersen SE. Concepts and principles in the analysis of brain networks. Ann N Y Acad Sci. 2011; 1224:126–146. [PubMed: 21486299]

Xu P, Huang R, Wang J, Van Dam NT, Xie T, Dong Z, Chen C, Gu R, Zang YF, He Y, et al. Different topological organization of human brain functional networks with eyes open versus eyes closed. Neuroimage. 2014; 90:246–255. [PubMed: 24434242]

Yeo BT, Krienen FM, Eickhoff SB, Yaakub SN, Fox PT, Buckner RL, Asplund CL, Chee MW. Functional Specialization and Flexibility in Human Association Cortex. Cereb Cortex. 2014

Yeo BT, Krienen FM, Sepulcre J, Sabuncu MR, Lashkari D, Hollinshead M, Roffman JL, Smoller JW, Zollei L, Polimeni JR, et al. The organization of the human cerebral cortex estimated by intrinsic functional connectivity. J Neurophysiol. 2011; 106(3):1125–1165. [PubMed: 21653723]

Zhang D, Snyder AZ, Fox MD, Sansbury MW, Shimony JS, Raichle ME. Intrinsic functional relations between human cerebral cortex and thalamus. J Neurophysiol. 2008; 100(4):1740–1748. [PubMed: 18701759]

Highlights

- Single-subject areal parcellation is reproducible, valid, and convergent with task
- Highly reliable correlation estimates require considerable data
- Within-subject correlation is most variable in visual and somatosensory cortex
- Individuals exhibit topological features distinct from group system organization

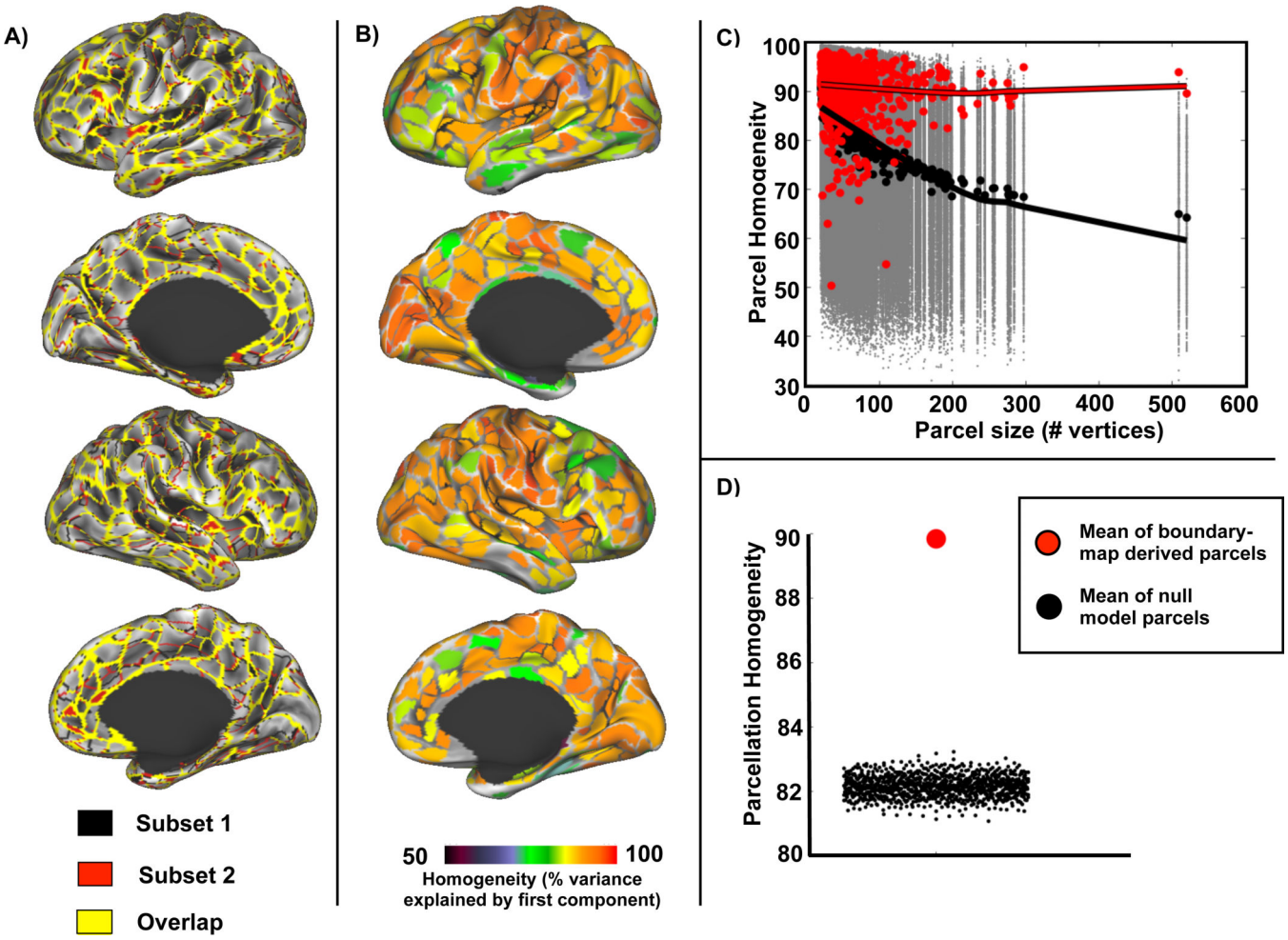

Figure 1.

Subject-specific parcellation is reproducible and internally valid. A) RSFC-based parcellation produces highly overlapping (yellow) parcel boundaries in two independent subsets of sessions (n = 42 per subset). B) Homogeneity of each parcel calculated as the percent of variance explained by the first eigenvector computed from PCA of the RSFC patterns from vertices in the parcel. C) Homogeneity of real parcels (red dots) by parcel size compared to homogeneity of null model parcels (gray dots). Black dots indicate median homogeneity across iterations for each null model parcel. Lowess fit lines highlight the effect of parcel size on homogeneity for the individual subject parcels (red line) and the null model parcels (black line). D) Mean homogeneity across parcels in the real parcellation (red dot) is significantly higher (Z-score = 23.1) than the mean homogeneity from null model parcellations (black dots).

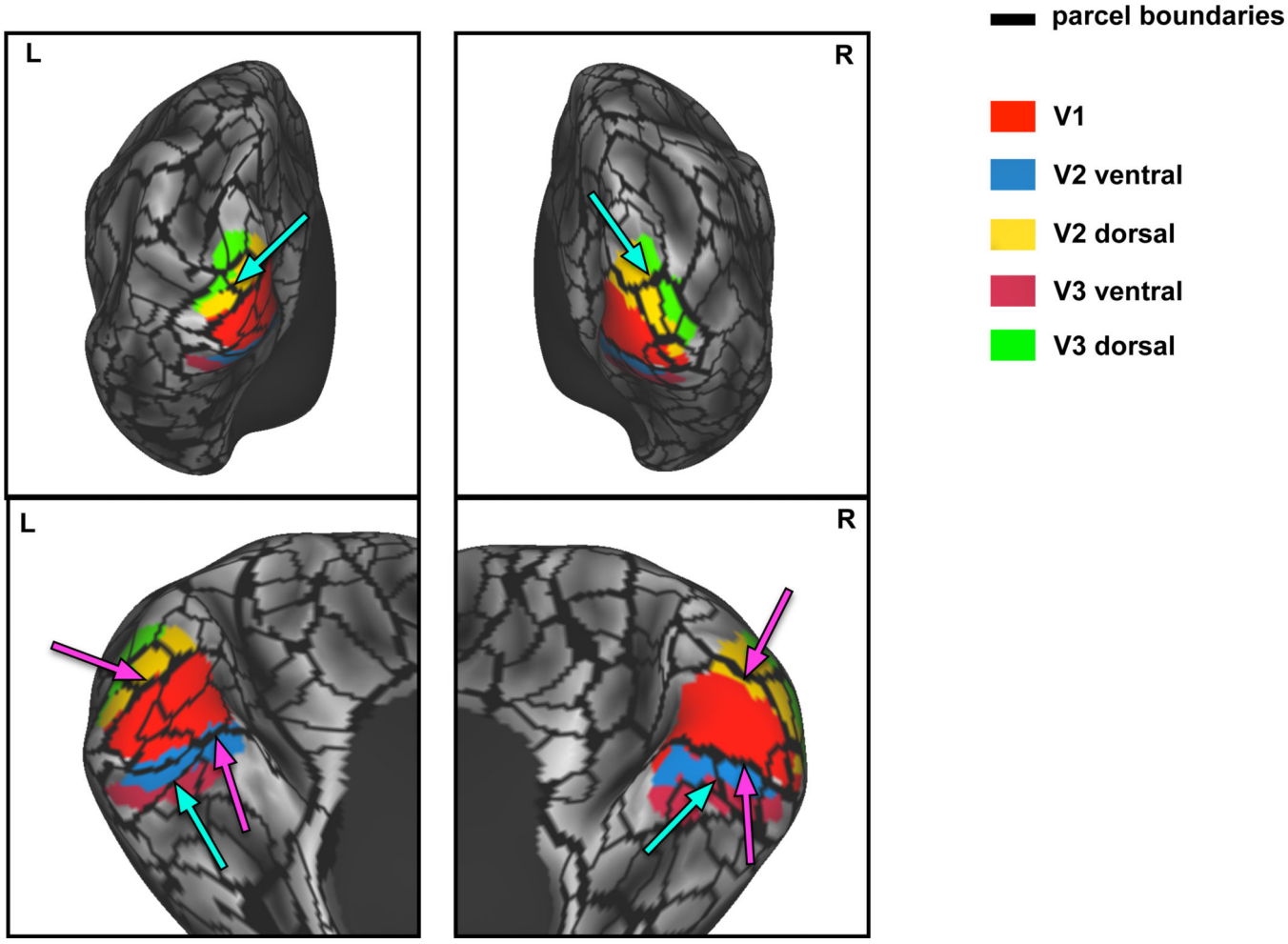

Figure 2.

Parcel boundaries defined in individual correspond with boundaries between retinotopically defined visual regions derived from the same subject. Magenta arrows indicate correspondence between the RSFC-based parcel boundaries and the boundary between V1 and V2 areas. Cyan arrows indicate RSFC-based parcel boundaries that may represent distinctions between foveal and peripheral representations in the visual field.

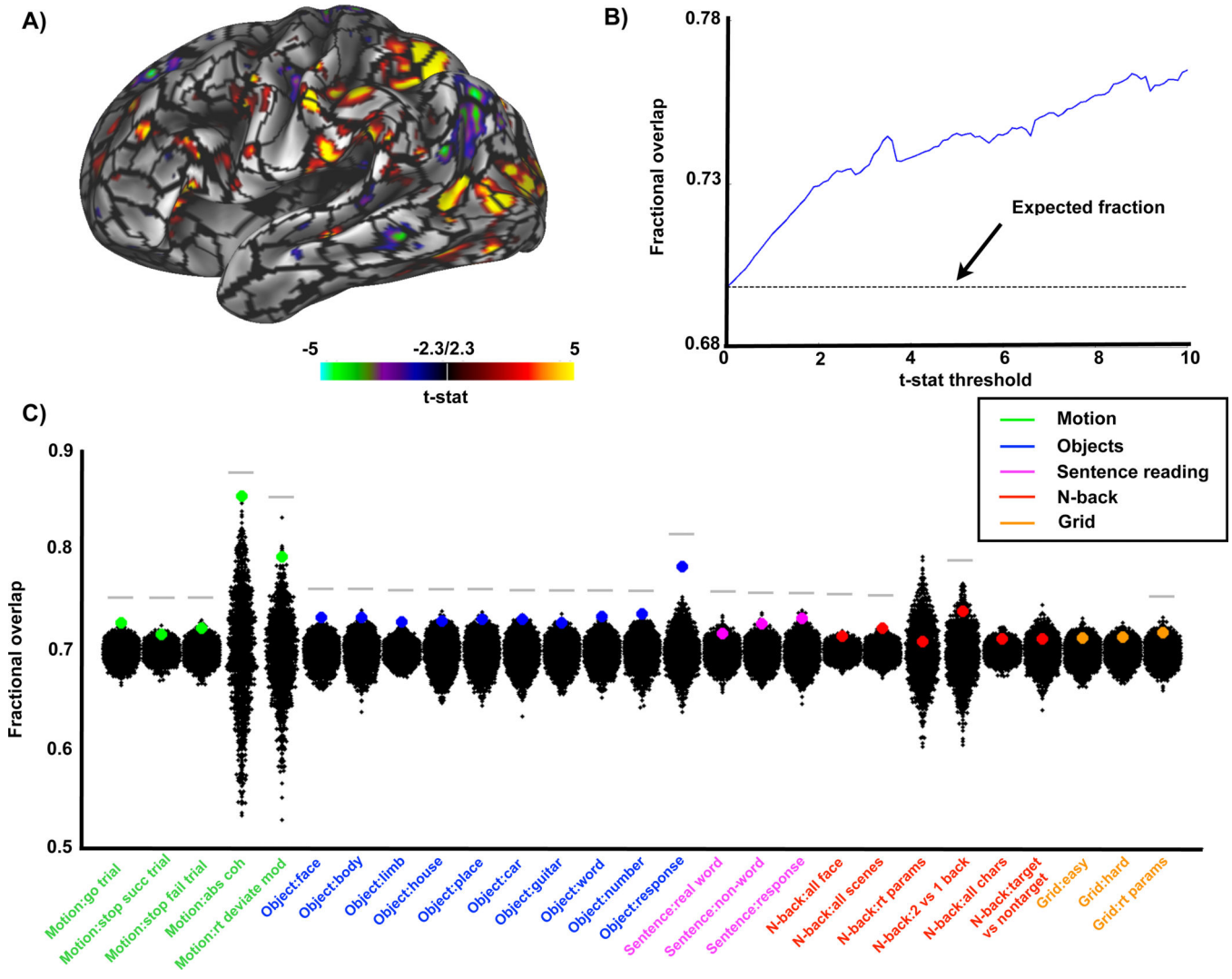

Figure 3.

RSFC-based parcellation corresponds with task activations. A) Parcellation boundaries overlaid on an example task contrast from the motion discrimination task. B) The average fraction of task-activated vertices that fall within parcels across all 27 task contrasts by t-stat threshold. Expected fraction by chance of task-activated vertices falling within parcel boundaries is 0.696 (dotted line). C) Each colored dot represents the fraction of task-activated vertices that fall within parcel boundaries for each task at a single t-statistic threshold (t=2.3) compared to a null model. The null distribution reflects task/parcel area overlap from rotated real parcel boundaries (black dots). Gray bar indicates real parcellation showed significantly more overlap with task-activated vertices than null parcellations ($p<0.05$).

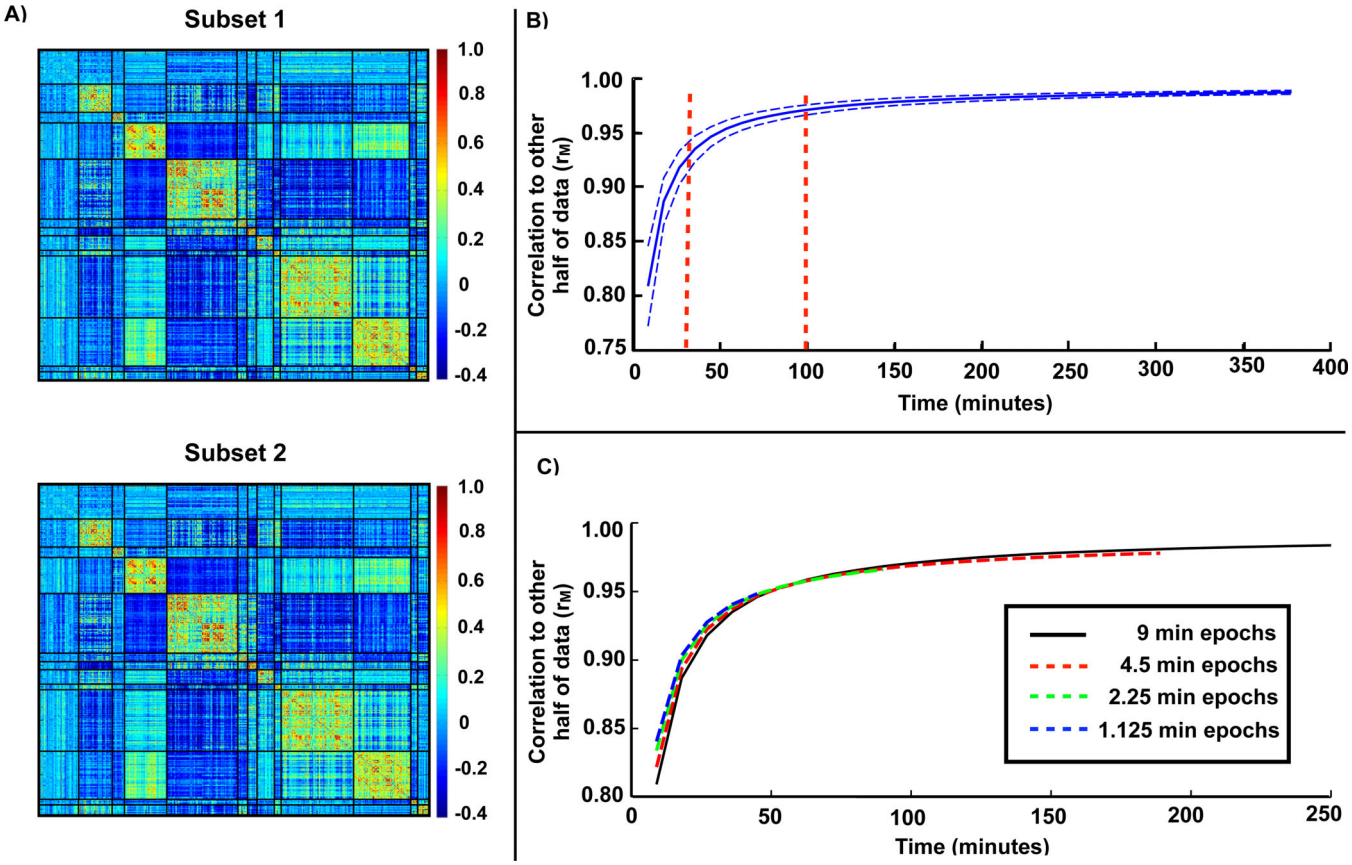

Figure 4.

Convergence of resting state correlation estimates requires significant amounts of data. A) Example parcel correlation matrices computed from each half of the data. The parcels are sorted by system with black lines indicating system boundaries (see Figure S1 for system assignments). B) Pearson correlation (r_M) of parcel-based correlation matrix from one half of the data with the correlation matrix generated from increasing amounts of data drawn from the other half. Represented are the mean (solid line) and standard deviation (dotted lines) of this correlation from 1000 random samplings of 84 sessions. C) Correlation when the same amount of time is drawn from a larger number of sessions, e.g. 18 minutes drawn from 4.5 minutes of 4 sessions (point on red line) is compared to 18 minutes drawn from 9 minutes of 2 sessions (point on black line).

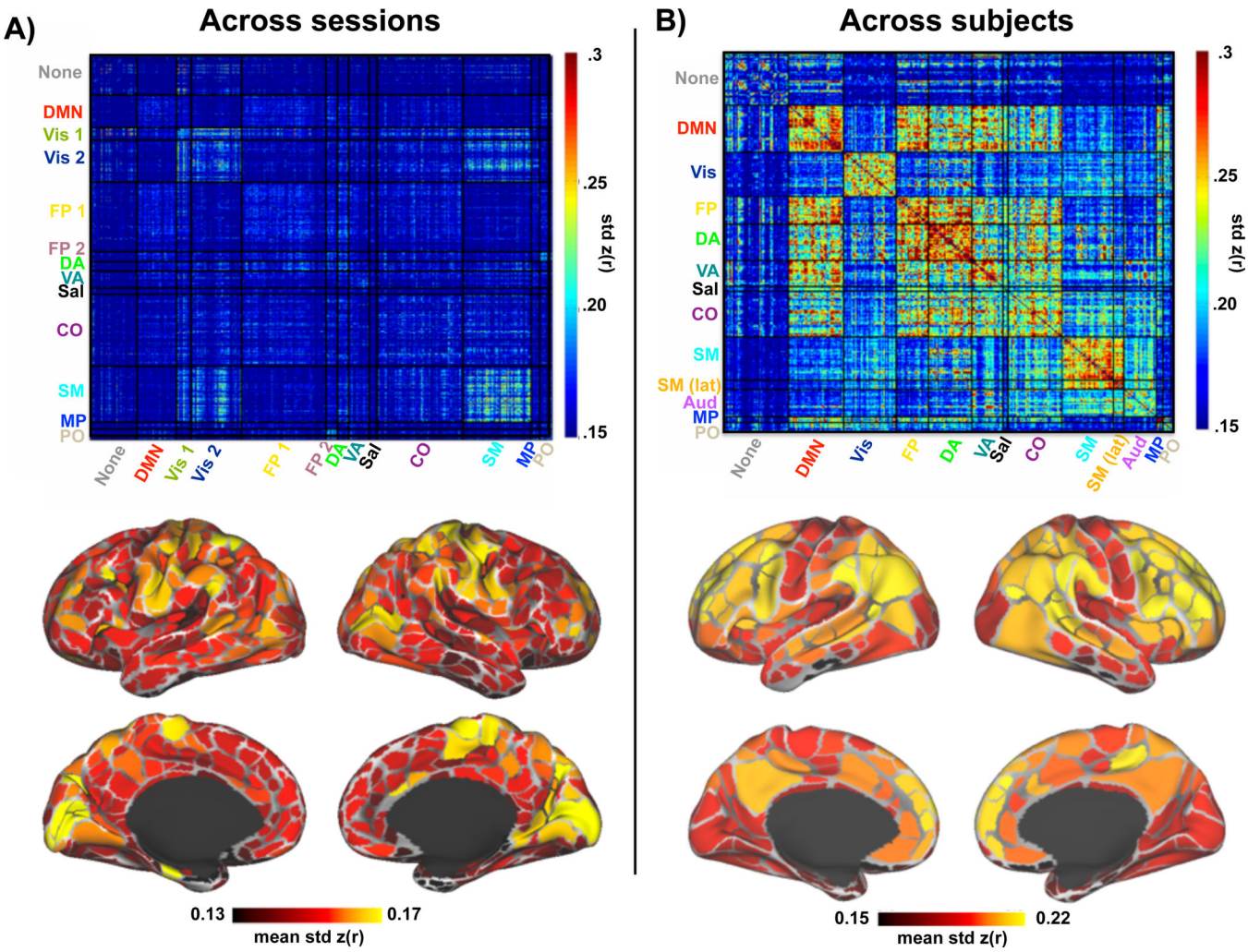

Figure 5.

Across-session compared to across-subject variability in resting state correlations. A) Above, parcel-to-parcel correlation standard deviation across sessions based on the individual subject parcellation and system assignment (see Figure S1). Below, the average correlation standard deviation for each parcel across all of its connections. B) Above, parcel-to-parcel correlation standard deviation across subjects using the group parcellation and system assignment reported in (Gordon et al., 2014b). Below, the average correlation standard deviation for each parcel across all of its connections.

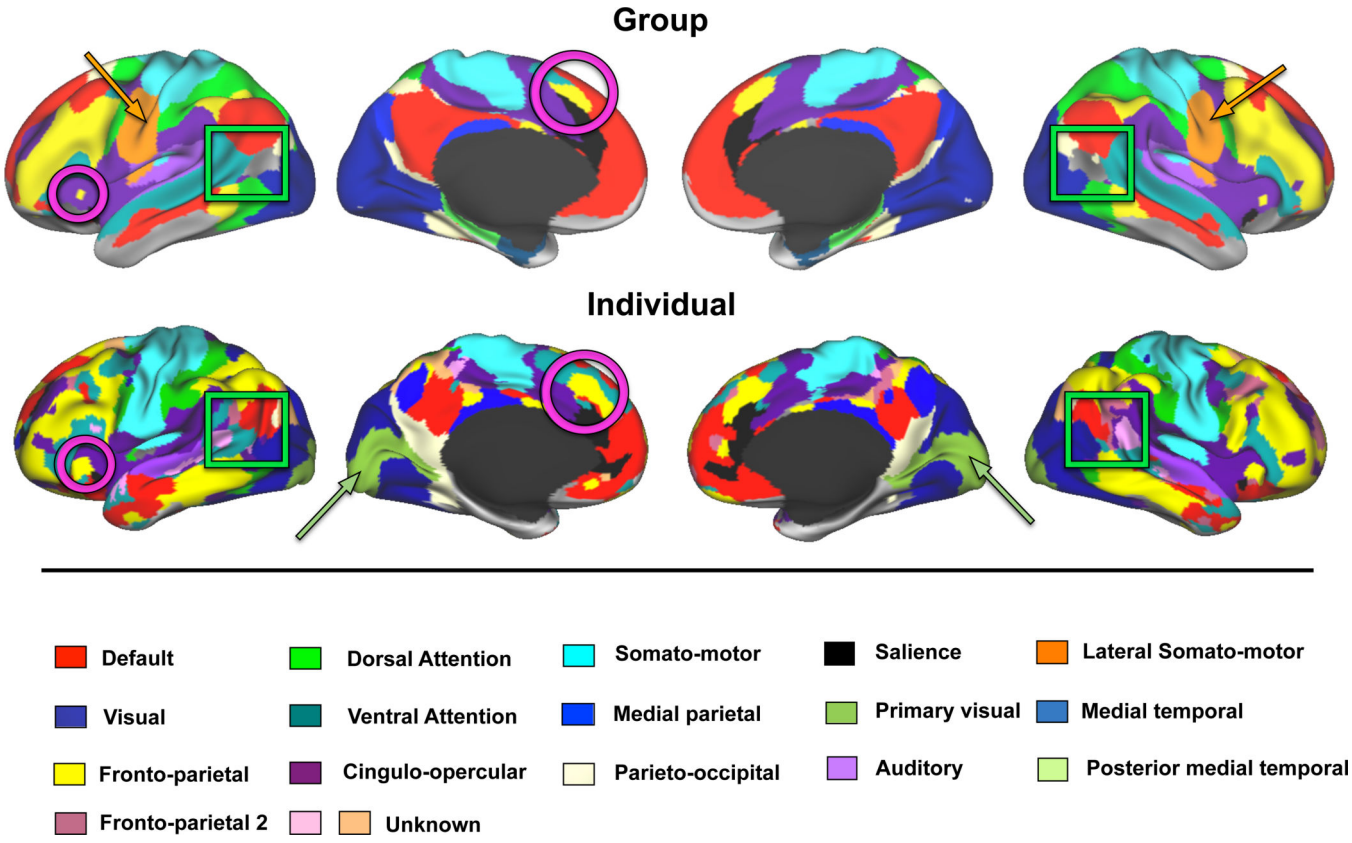

Figure 6.

Primary subject Infomap-based community detection produces resting state community topology similar to a 120-subject group average dataset. The maps depicted here represent a single view of community identity collapsed across multiple edge density thresholds (additional edge densities are found in Figure S5). Magenta circles highlight similarities between the individual and the group in the fronto-parietal system. Orange arrows point to the lateral somato-motor system present in the group but not the individual, while olive arrows point to the primary visual system present in the individual but not the group.

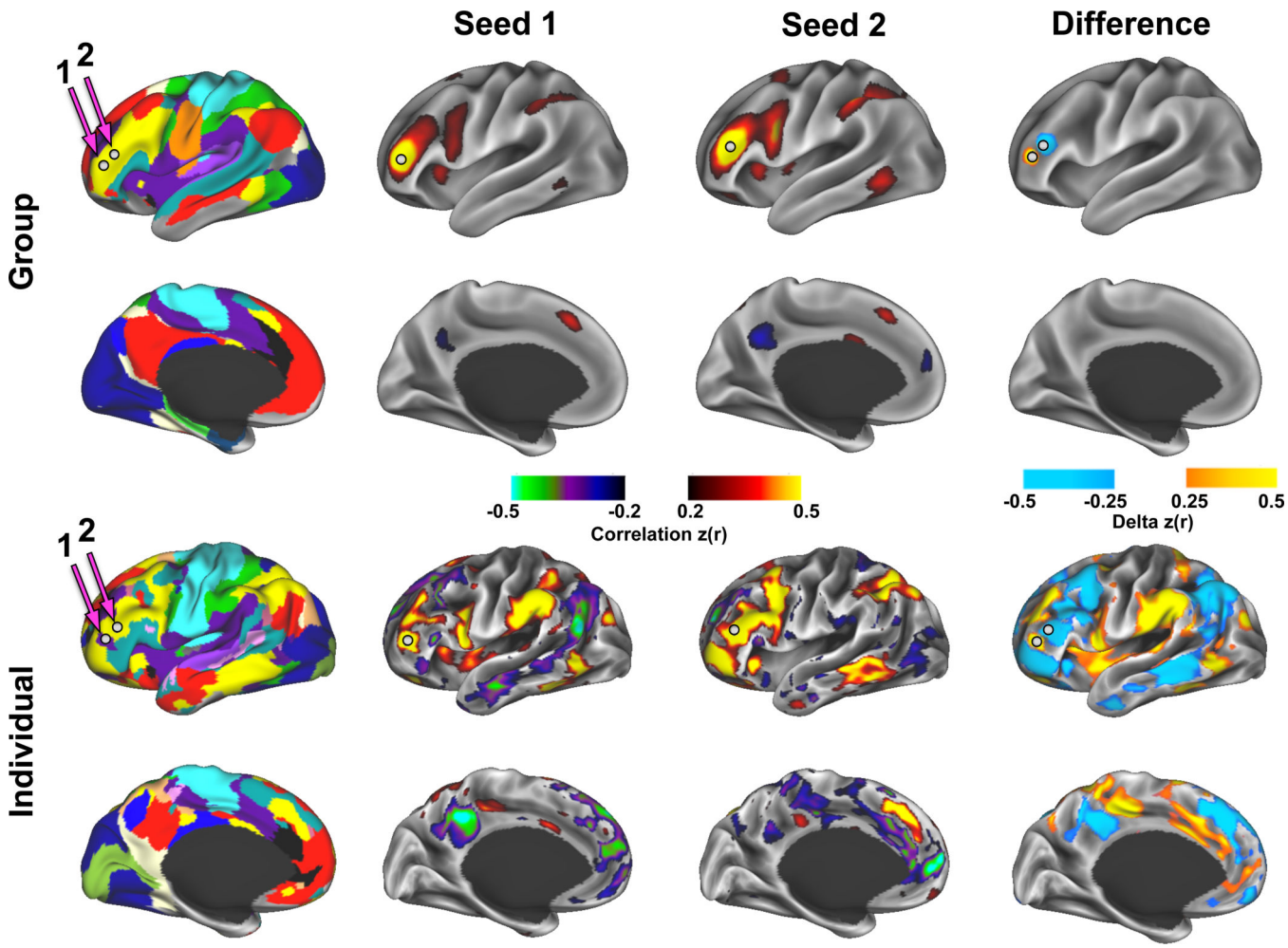

Figure 7.

Example of idiosyncratic patterns of functional connectivity in an individual. Two nearby regions of interest (white spheres) in the lateral frontal cortex have the same system identity in the group (fronto-parietal) but different system identities in the individual (cingulo-opercular and fronto-parietal). Above, correlation maps from these two regions have very similar patterns in the group, with the largest differences occurring locally. Below, The same two regions demonstrate starkly different correlation patterns in the individual, with large regions of cortex showing large differences in correlation.